Available online at www.sciencedirect.com
ScienceDirect
International Journal of Heat and Mass Transfer 49 (2006) 5001–5009
International Journal of HEAT and MASS TRANSFER
www.elsevier.com/locate/ijhmt

A numerical model for the analyses of heat transfer and leakages in a rotary air preheater

Boštjan Drobnič, Janez Oman *, Matija Tuma

Faculty of Mechanical Engineering, University of Ljubljana, Aškerčeva 6, 1000 Ljubljana, Slovenia

Received 5 October 2005
Available online 22 August 2006

Abstract

Air preheaters make a considerable contribution to the improved overall efficiency of fossil-fuel-fired power plants. In this study we used a combination of fluid dynamics and a newly developed three-dimensional numerical model for heat transfer as the basis for a theoretical analysis of a rotary air preheater. The model enables studies of the flue-gas flow through the preheater and the adjoining channels as well as the regenerative heat transfer and the resulting temperature distribution in the matrix of the preheater. Special attention was focused on the influences of leakages on the flue-gas parameters in the preheater. The numerical analysis and the experimental results showed an obvious dependence of the flue-gas parameters on various seal settings. Based on the results a method for online monitoring of the tightness of the radial seals is proposed.

Keywords: Regenerative heat transfer; Rotary air preheaters; Sealing; Leakages; Numerical simulation; CFD

1. Introduction

High efficiency is the key feature in the operation of any energy-conversion device, and this includes large fossil-fuel-fired steam boilers. It is therefore very important to recover as much energy as possible from that available in the fuel. Air preheaters have proved to have an important influence on the efficiency of the entire steam boiler. Their primary task is to return considerable amounts of waste heat, carried by the flue gas, back to the combustion process. Due to their compactness and high performance, rotary regenerative air preheaters are very common in fossil-fuel-fired steam boilers. Rotary preheaters have a specific operating principle where the heat is transferred from the flue gas to the air by means of a rotating matrix. A significant weakness of this type of heat exchanger is the unavoidable leakages between both streams caused by the pressure difference between the streams and by the rotation of the matrix. At the same time there is a need for the constant monitoring of the seals' settings in order to ensure their optimum operation under various working conditions.

An efficient sealing system is therefore a prerequisite for the high performance of an air heater and, consequently, the high efficiency of the steam boiler. The main side effect of the leakage is the need for larger flow rates of air entering the heater and, consequently, larger flow rates of flue gas exiting the heater. The increased flow rates also require more ventilation power.

This article presents a method that makes possible the online monitoring of the air preheater's seal tightness. The method is based on the results of numerical simulations. A numerical method was developed that makes it possible to simulate the operation of the rotary air preheater, including the influences of various seal settings on the properties of the flue gas after the preheater. The numerical results were confirmed by measurements.

* Corresponding author. Tel.: +386 1 477 1306; fax: +386 1 251 8567.
E-mail address: janez.oman@fs.uni-lj.si (J. Oman).

0017-9310/$ - see front matter © 2006 Elsevier Ltd. All rights reserved.
doi:10.1016/j.ijheatmasstransfer.2006.05.027

Nomenclature

c	specific heat, J/kg K
i	index in radial direction
j	index in tangential direction
k	index in axial direction
N	number of grid divisions
r	radial coordinate, m
T	temperature, °C
w	velocity, m/s
z	axial coordinate, m

Greek symbols

α	convective heat-transfer coefficient, W/m^2 K
β	heat-transfer surface in unit volume of matrix, m^2/m^3
θ	tangential coordinate, rad
λ	thermal conductivity, W/m K
ρ	density, kg/m^3
σ	solid fraction of matrix volume, m^3/m^3
φ	solid fraction of matrix cross-section, m^2/m^2
ω	rotational speed, rad/s

Subscripts

amb	ambient
g	gas
m	matrix
p	constant pressure

2. Leakages in rotary heat exchangers

The basic element of a rotary heat exchanger's operation is a rotating matrix in a compact casing that transfers the heat from the hot flue gas to the cold combustion air. The rotation of the matrix requires an appropriate sealing system to prevent mixing of the flue gas and the air, commonly referred to as leakage. The importance of sealing and leakage and its influence on air-preheater performance was studied by several authors. MacDuff and Clark, for example, present an overview of radial sealing systems [1]. A lot of research was carried out by Skiepko, who studied the influence of leakage on a heat exchanger's performance [2]. He also presented methods for calculating the mass flows of gas through the seals [3], a method of measuring and adjusting the seal clearances in radial seals [4–6], and the irreversibilities caused by leakage [7]. The general conclusion is that the sealing system is an important part of a rotary heat exchanger. Although the leakages in the air preheater do not significantly affect the boiler's overall thermal efficiency [8], excessive leakages can reduce the effectiveness of the air preheater itself by over 10% [2]. At the same time, leakages require more air to be transported to the preheater and more flue gas to be transferred from the preheater, and larger quantities of gases require more power for the air and flue-gas fans. These fans typically use up to 1.5% of all the power produced. An increased amount of power required for the fan results directly in a noticeable drop in the power plant's overall efficiency. It is therefore important to pay special attention to the adjustment of the seals and to monitor their tightness.

Fig. 1 schematically shows a typical arrangement of seals around the rotor of a rotary heat exchanger. The three types of seals in Fig. 1 prevent leakage due to pressure differences between certain locations in the heat exchanger.

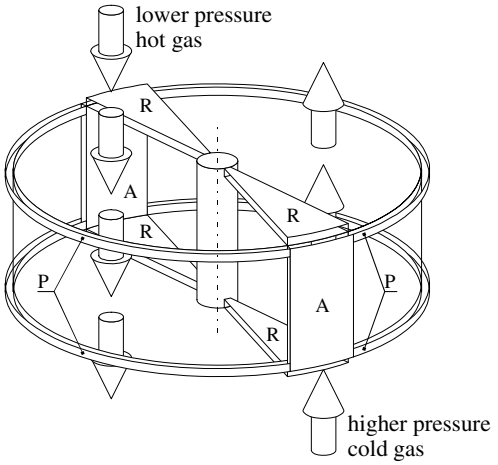

Fig. 1. Typical arrangement of the seals in a rotary heat exchanger (A – axial seals, P – peripheral seals, R – radial seals).

Radial and axial seals reduce the amount of air that is leaking into the flue-gas channel. Typically, the pressure on the air side is considerably higher than the pressure of the flue gas: the difference can reach several thousand Pa. Peripheral seals, on the other hand, prevent the bypass flow of air or flue gas around the matrix. This flow does not contribute to the heat exchange and should also be reduced.

Mass flow rates through the peripheral seals are relatively small since the pressure gradients in the axial direction are much smaller than the pressure difference between the hot and cold gas streams. The axial seals are usually several times shorter than the radial seals, so the majority of the gas is expected to pass through the radial seals.

Both the radial and axial seals are adjustable. During start-up or after changing the boiler's load the rotor is deformed due to temperature differences at the hot and cold ends of the rotor. The seals need to be adjusted after any change in the temperature conditions in the exchanger.

Therefore, a suitable means of monitoring the sealing quality should be provided.

In rotary heat exchangers another type of leakage occurs, i.e., carry-over leakage. This carry-over leakage means there is always some gas, hot or cold, caught within the matrix's empty space as it moves from one stream to another, which means it is transferred to the opposite stream. The carry-over leakage can be reduced by an appropriate design of the air preheater and the adjoining air and flue-gas channels.

3. Numerical analysis

The effects of various radial-seal settings on the flue-gas properties after an air preheater have been theoretically researched using a numerical model. The model is a combination of fluid-flow simulation and heat-transfer simulation in a three-dimensional geometrical model of a rotary regenerative heat exchanger.

The fluid-flow simulations are based on solving a system of transport equations, which is done with commercial CFD software. An new, additional model was used to simulate regenerative heat transfer within the matrix of the heat exchanger.

3.1. Heat-transfer model

The CFD analysis produces a three-dimensional flow field in the computational domain. While most of the heat-transfer models proposed by several authors are only two-dimensional, a three-dimensional model must be used in this case. The benefits of three-dimensional analyses were discussed by Franković [9], so a similar three-dimensional heat-transfer model was developed for analysing the operation of an air preheater. The model is based on energy conservation in a differential control volume, as shown in Fig. 2. The use of a cylindrical coordinate system is suggested by the cylindrical shape of the matrix and its rotational motion.

There are five heat fluxes entering the control volume as well as five heat fluxes exiting the control volume (see Fig. 2). All of them are combined into a single heat-balance equation for a differential control volume:

$$w_g\rho_g c_p(1-\varphi_z)\frac{\partial T_g}{\partial z}+\omega\sigma_m\rho_m c_m\frac{\partial T_m}{\partial\theta} - \lambda\left[\varphi_z\frac{\partial^2 T_m}{\partial z^2}+\varphi_\theta\frac{1}{r^2}\frac{\partial^2 T_m}{\partial\theta^2}+\varphi_r\left(\frac{1}{r}\frac{\partial T_m}{\partial r}+\frac{\partial^2 T_m}{\partial r^2}\right)\right] = 0 \quad (1)$$

The first term on the left-hand side of Eq. (1) represents the heat conveyed by the gas, the second term represents the heat conveyed by the matrix, and the entire third term on the left-hand side represents the heat conduction in the matrix material in all three coordinate directions. Parameters φ_r, φ_θ and φ_z are the fractions of solid material in the matrix cross-section in the respective directions.

Besides heat convection and conduction through the control volume there is also heat transfer from the gas to the matrix, or vice versa, taking place within the control volume. The heat transfer is described with the following equation:

$$-w_g\rho_g c_p(1-\varphi_z)\frac{\partial T_g}{\partial z}-\alpha\beta(T_g-T_m)=0 \quad (2)$$

The first part on the left-hand side is the heat flux to or from the air or flue gas, and the second part is the heat flux to or from the matrix. The coefficient β represents the heat transfer surface in a unit volume of the matrix.

For the purpose of the numerical simulation, Eqs. (1) and (2) are combined and expressed in terms of finite differences instead of partial derivatives. This yields the expression

$$\begin{aligned}&\alpha\beta T_m(i,j,k)-\alpha\beta T_g(i,j,k)+\omega\sigma_m\rho_m c_m \times\frac{T_m(i,j,k)-T_m(i,j-1,k)}{\Delta\theta} \\ &-\lambda\varphi_z\frac{T_m(i,j,k+1)-2T_m(i,j,k)+T_m(i,j,k-1)}{\Delta z^2} \\ &-\frac{\lambda\varphi_\theta}{r^2}\frac{T_m(i,j+1,k)-2T_m(i,j,k)+T_m(i,j-1,k)}{\Delta\theta^2} \\ &-\frac{\lambda\varphi_r}{r}\frac{T_m(i,j,k)-T_m(i-1,j,k)}{\Delta r} \\ &-\lambda\varphi_r\frac{T_m(i,j,k+1)-2T_m(i,j,k)+T_m(i,j,k-1)}{\Delta r^2} \\ &=0\end{aligned} \quad (3)$$

The transformation is done by employing standard numerical methods for parabolic partial differential equations. Since rotational speed of the rotor is constant time coordinate that is commonly used was replaced by rotational angle θ. The implicit scheme was used with the first order derivatives to ensure stability of the model [10].

The computational domain is covered with a grid that coincides with the cylindrical coordinates r, θ and z. Each grid point is described with the indices i, j and k, which describe its radial, tangential and axial positions, respectively. Boundaries and respective index values are shown

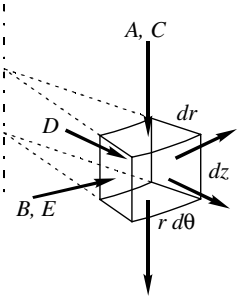

Fig. 2. Heat fluxes through a differential control volume (A – heat carried by gas; B – heat carried by matrix; C, D and E – heat conducted through matrix material in axial, radial and tangential directions, respectively).

Table 1
Boundaries of computational domain and respective index values of numerical model

Boundary	Index value
Inner wall of the rotor	$i = 0$
Outer wall of the rotor	$i = N_r$
Starting angle of current regeneration phase	$\theta = 0$
Ending angle of current regeneration phase	$\theta = N_\theta$
Gas inlet surface	$z = 0$
Gas outlet surface	$z = N_z$

in Table 1. The matrix temperature at any point (i,j,k) can be calculated using Eq. (3).

The heat-transfer coefficient, α, depends on the properties of the gas; the model allows it to have a constant or variable value. Thorough investigations of the dependence of the heat-transfer coefficient on other gas properties were published Stasiek et al. [11,12]. Their findings were used to define the heat-transfer coefficient in terms of the Reynolds number for the presented simulations.

Since two unknown temperatures are sought for each computational point, the temperature of the matrix and the temperature of the gas, the solution can only be achieved iteratively. Several boundary conditions must also be set in order to enable an iterative simulation of the heat transfer using the model represented by Eq. (3).

At the boundaries of the computational domain matrix temperatures with indices less than 0 or more than N_r, N_θ or N_z are required in Eq. (3). Since these values do not exist their virtual values are defined with several boundary conditions:

- radial direction
  - inner wall $(i = 0)$ is adiabatic: $T_m(-1,j,k) = T_m(0,j,k)$,
  - heat loss through outer wall $(i = N_r)$ with known (estimated) heat-transfer coefficient α_{amb} towards the ambient air: $T_m(N_r + 1,j,k) = T_m(N_r,j,k) - \Delta r \frac{\alpha_{amb}}{\lambda_g}(T_m(N_r,j,k) - T_{amb})$,
- tangential direction – temperatures are transferred from the previously calculated side of the heat exchanger
  - matrix entering computational domain $(j = 0)$: $T_m(i,-1,k) = T_m^+(i,N_\theta,N_z - k)$,
  - matrix exiting computational domain $(j = N_\theta)$: $T_m(i,N_\theta + 1,k) = T_m^+(i,0,N_z - k)$, (+ denotes results from the previously calculated side of the preheater),
- axial direction – both inlet and outlet surfaces are adiabatic
  - gas inlet $(k = 0)$: $T_m(i,j,-1) = T_m(i,j,0)$,
  - gas outlet $(k = N_z)$: $T_m(i,j,N_z + 1) = T_m(i,j,N_z)$.

Eq. (3) and the above boundary conditions form the numerical model that was used for simulations of the temperature distribution within the matrix of a rotary air preheater.

3.2. Geometrical model of an air preheater

The computational domain for the CFD simulations included the flue-gas section of the air preheater's rotor as well as a part of the inlet and outlet channels, as depicted in Fig. 3.

The dimensions of the simulated air preheater (Table 2) are comparable to an existing, real-air preheater on which measurements were performed in order to confirm the results from the numerical simulation.

The boundary conditions were also set to be similar to real conditions in order to achieve comparability between the numerical and measurement results. The numerical model was applied to six cases in which only the radial seals' settings were varied. All the radial seals were set as an inlet boundary condition with a specified mass flow. The mass flow was determined with respect to the pressure

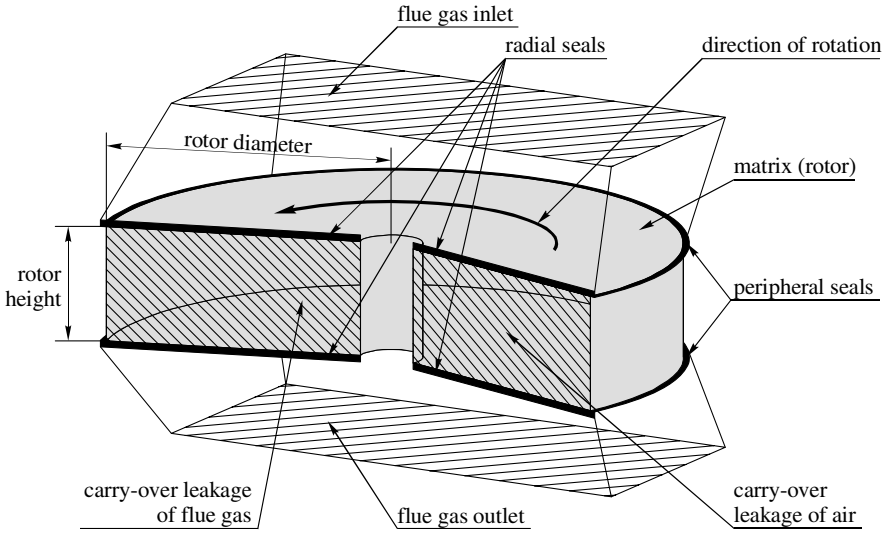

Fig. 3. Computational domain with boundary surfaces.

Table 2
Dimensions of the air preheater in the numerical simulation

Rotor outer radius (m)	4.6
Rotor height (m)	1.8
Inlet/outlet channel width (m)	8.0
Inlet/outlet channel depth (m)	3.6
Inlet/outlet channel – rotor joining piece height (m)	1.7

differences between the flue gas and the air in the channels, and the seal clearance. In the first case all the seal clearances were equal. For the second case all the seal clearances were doubled to achieve the effect of non-optimised seal settings. In each of the other four cases only one of the clearances was doubled, while the others were left at their initial setting from the first case.

3.3. Results of the numerical simulation

The final results of the CFD simulation, customized with the described heat-transfer model, are three-dimensional distributions of the flue-gas velocity, the temperature and the fraction of CO_2 in the flue gas over the entire computational domain. Measurements of the flue-gas properties for the calculation of the boiler's efficiency should take place after the air preheater, Fig. 8. The results of the numerical simulations are therefore also presented on the flue-gas outlet surface, Fig. 3. The results show the expected values of particular flue-gas properties at any location on the outlet surface.

Fig. 4 shows the temperature and the distribution of the fraction of CO_2 at the outlet surface for the case of small clearances for all the radial seals. Both parameters have very high gradients at the inner edge of the surface. This is caused by irruption of the air that usually has a considerably higher pressure than the flue gas into the flue-gas channel.

If the seal clearances are increased, more air rushes into the flue-gas channel and, consequently, both the temperature and the fraction of CO_2 at the inner wall of the outlet channel decrease. Fig. 5 shows the temperature and the distribution of the fraction of CO_2 for the second case, where all four radial seals had increased clearances.

The main difference in the distributions of the temperature and the fraction of CO_2 occurs at the edge of the channel cross-section that is closer to the axis of rotation. Therefore, a sampling line was set at about 0.2 m from the edge of the channel. The temperatures and CO_2 fractions on the sampling line are compared in Fig. 6 for the initial case (thin black line) and for the four cases where each of the radial seals' clearance was increased

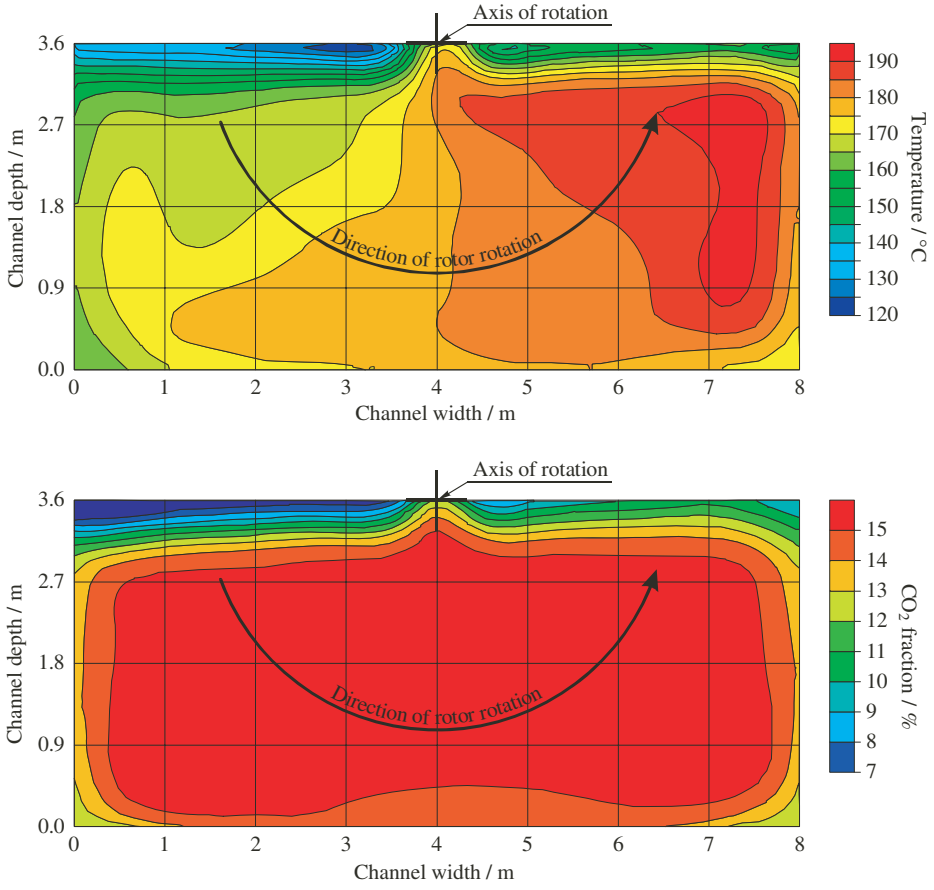

Fig. 4. Temperature and distribution of the fraction of CO_2 on the flue-gas outlet surface of a rotary air preheater with the initial setting of the radial seals.

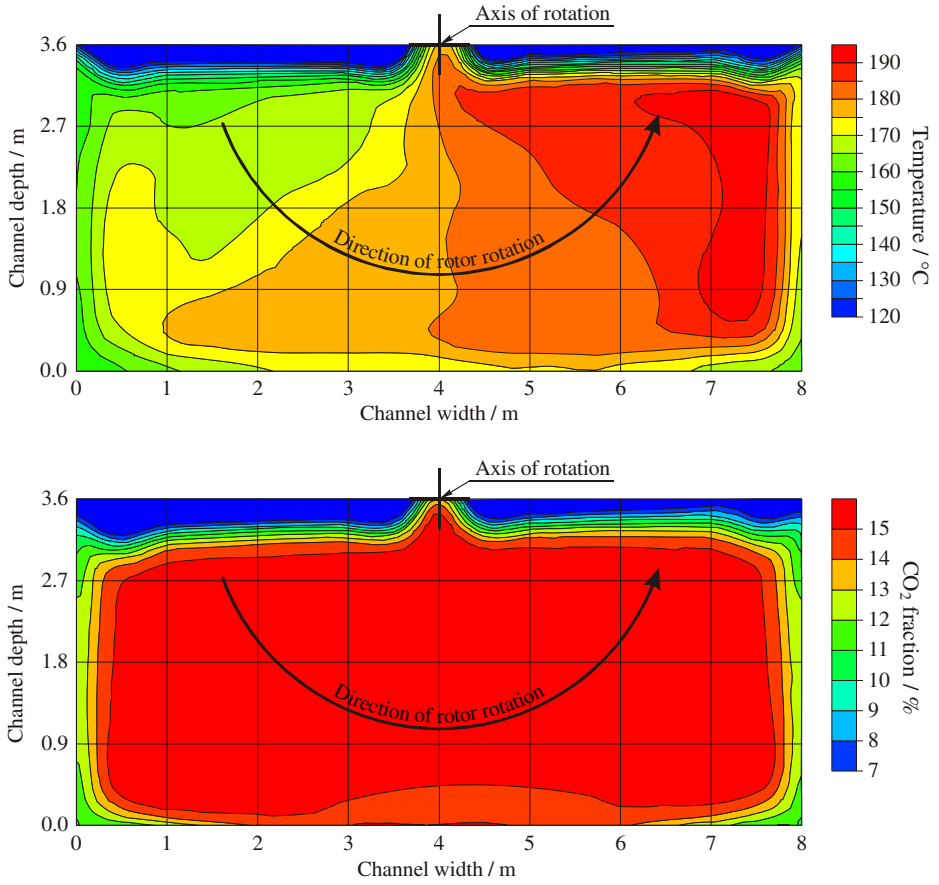

Fig. 5. Temperature and distribution of the fraction of CO_2 on the flue-gas outlet surface of a rotary air preheater with increased radial seal clearances.

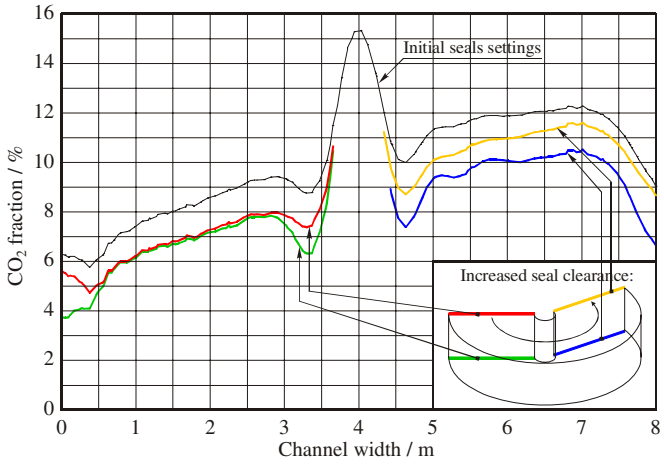

Fig. 6. Calculated distribution of CO_2 fraction along the inner wall of the flue-gas channel.

individually (coloured lines).[1] Since the left- and right-hand side seals only affect their respective sides of the channel, only half of the lines are drawn for these cases.

Obviously, the increased seal clearance affects the fraction of CO_2, which is decreased for all four cases. It is possible to determine whether the increased leakage occurred at the left- or right-hand side of the rotor. But it is not possible to distinguish the leakages through the seals at the hot end and the cold end of the rotor.

The air that is mixed with the flue gas at the hot end of the rotor has a much higher temperature than the air that is

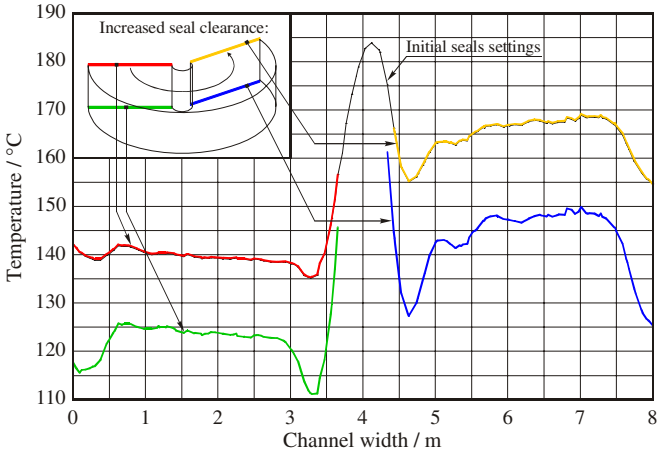

Fig. 7. Calculated distribution of temperature along the inner wall of the flue-gas channel.

[1] For interpretation of color in Figs. 6 and 7, the reader is referred to the web version of this article.

mixed at the cold end. The temperature of the flue gas at the sampling line should therefore depend on whether the leakages are increased at the hot or cold end of the rotor. The numerical simulation confirmed these assumptions, as is shown in Fig. 7. The increased leakage at the cold end significantly lowered the flue-gas temperature (the green and blue lines in Fig. 7). On the other hand, the increased leakage at the hot end has virtually no effect on the flue-gas temperature. The red and yellow lines in Fig. 7 practically coincide with the thin line representing the initial setting of the radial seals.

4. Measurements

In order to confirm the theoretical results of the numerical simulation, measurements were performed on an existing air preheater. The measurements took place in a 275-MW pulverized-coal-fired power plant in Slovenia. Two identical rotary air preheaters provided the hot air for the combustion process, which represents approximately 80% of the total combustion-air flow rate.

The dimensions of the preheater roughly match those of the numerically analysed preheater. The rotor diameter and height are 9358 mm and 1775 mm, respectively. The construction of the preheater and the adjoining channels did not make it possible to make measurements on the same plane that was analysed numerically. As a result, the measuring plane was further down the flue-gas channel, as shown in Fig. 8.

A combined probe for simultaneous measuring of the temperature, the gas composition and the velocity was designed for the presented measurements [13]. Both measuring instruments for the temperature and the CO_2 fraction have a measuring error within $\pm 0.1\%$ of full scale. The properties of the flue gas were only measured at a single point with the probe, so a series of measurements had to be performed to cover the entire measuring plane. Due to the repositioning of the probe and the large dimensions of the flue-gas channel the errors in identifying the exact location of the probe were bigger than the errors of the measuring instruments.

The same measuring procedure was performed before and after a general overhaul of the air preheater, at which time the sealing system was also improved. The measurements before the overhaul therefore represent the case of an improper seal setting, while the measurements after the overhaul represent the case of a tight seal setting.

4.1. Measuring procedure

The flue-gas properties were measured at 42 points over a cross-section of the preheater's outlet channel, Fig. 8, according to VDI guidelines [14]. The entire series of measurements took approximately 2 hours. During this time all the operating parameters of the power plant were kept at constant levels.

The locations of all the measuring points on the measuring plane are shown on the right-hand side of Fig. 8. The results from all 42 measuring points give distributions of the flue-gas properties over the entire measurement plane. A detailed presentation of the measuring methods and results can be found in [15].

The seven measuring points on the sampling line (right-hand side of Fig. 8) were used for a comparison with the numerical results in Figs. 6 and 7. The distance of the sampling line from the channel's wall is approximately 0.2 m, while the distance between the neighbouring points is 1.2 m.

4.2. Results and discussion

A comparison of the numerical and experimental results is shown in Fig. 9. Obviously, both results follow the same principles. Both the fraction of CO_2 and the temperature increase from the left-hand side towards the right-hand side of the channel. There is also a noticeable drop in both parameters at the left- and right-hand edges of the channel.

On the left-hand side of the channel the fraction of CO_2 is smaller due to additional air that is being carried over

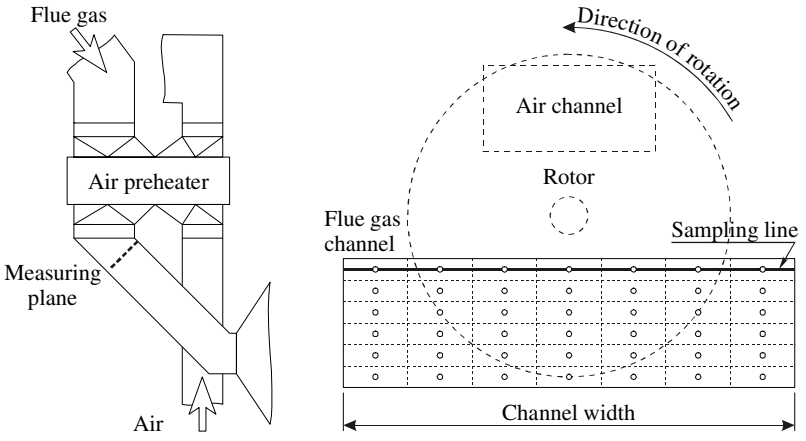

Fig. 8. Positions of the measuring plane, the measuring points and the sampling line in the flue-gas outlet channel.

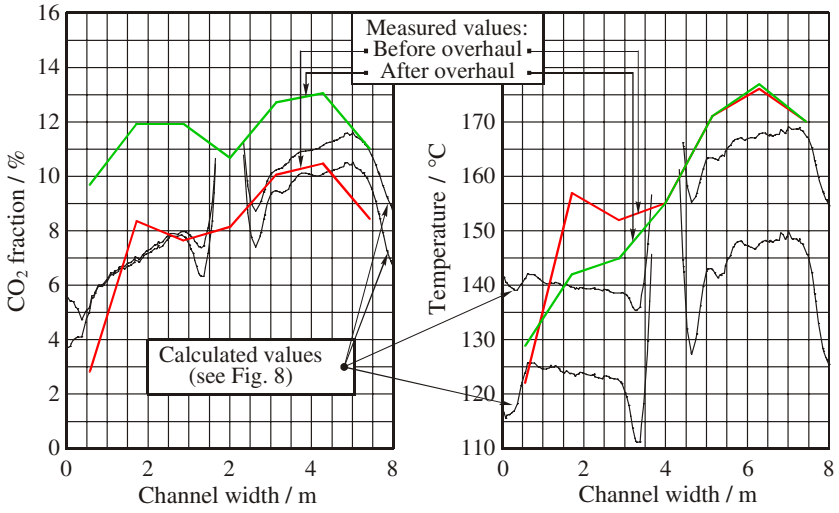

Fig. 9. Measured values of CO_2 fraction and flue-gas temperature along the inner wall of flue-gas channel compared to calculated values.

from the air channel with the rotor matrix. In the middle of the channel almost pure flue gas is observed in the numerical simulation since no leakage is simulated at the rotor axis.

The left-hand diagram in Fig. 9 shows an increase in the fraction of CO_2 by 1.5–2% after the overhaul. This clearly indicates that a lot less air is being mixed with the flue gas. The noticeable difference between the profiles shown in Figs. 4 and 5 already showed the significant effect that the amount of air that is being mixed with flue gas has on the distribution of the fraction of CO_2. If only one of the four radial seals has an increased clearance the differences are smaller, but still noticeable, and they only appear on the side of the channel where the increased leakage occurs.

The new sealing system performs a lot better than the old one. However, the right-hand diagram in Fig. 9 shows very little change in the temperature of the flue gas. The numerical simulation showed that increased leakages at the hot end, the left- and the right-hand sides of the rotor had virtually no effect on the flue-gas temperature, Fig. 7. On the other hand, increased leakages at the cold end noticeably reduced the flue-gas temperature. The findings of the numerical simulation therefore lead to the conclusion that the majority of the leakage taking place before the overhaul occurred at the hot end of the rotor. This is because it is common to have a lot of abrasion damage at the hot end of air preheaters' rotors. The abrasion is caused by the particles of ash that are carried by the flue gas flowing through an air preheater. This damage is the most likely cause of the increased leakage.

Both the numerical and experimental results show that combined measurements of the fraction of CO_2 and the temperature at the inner wall of the flue-gas outlet channel make it possible to accurately detect which of the four radial seals is not optimally set. It is necessary, though, to know the temperatures and the fractions of CO_2 at the sampling points for the optimal seal setting. In other words, the thinner line in Figs. 6 and 7 needs to be known.

For online monitoring of the radial-seal settings at least two pairs of probes need to be installed in the flue-gas outlet channel. With respect to the results of the numerical simulation and the measurements, the proposed areas where the measuring probes should be positioned are shown in Fig. 10. The actual shape and size of the areas might vary for preheaters with different geometries of the flue-gas channels. But in general the measuring probes should be placed in the left- and right-hand parts of the channel near the wall of the channel that is closest to the axis of matrix rotation.

Each pair of probes consists of a probe for measuring the temperature and one for measuring the fraction of CO_2. The measurement results need to be compared to the results of an initial setting to provide an estimation of the radial seals' tightness or the distribution of leakages among all four radial seals. An increased fraction of CO_2 indicates a reduced tightness of the sealing on the

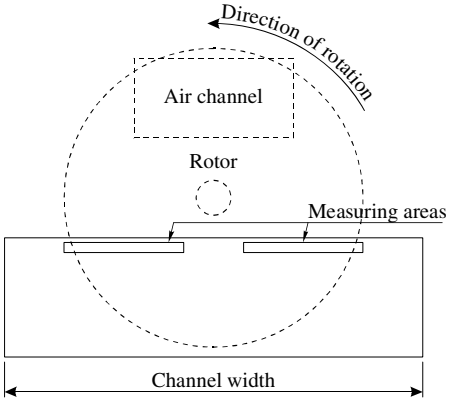

Fig. 10. Proposed areas for positioning the measuring probes for online monitoring of the radial-seals' tightness.

respective side of the rotor. The change in temperature can further indicate whether the increased leakage occurs at the hot or the cold end of the rotor.

5. Conclusions

The importance of an appropriate radial-seal tightness in rotary regenerative air preheaters requires a suitable method for monitoring the seal settings. To study the effects that various seal settings have on the flue-gas properties a new numerical heat-transfer model was developed. The model enables three-dimensional flow and heat-transfer simulations within any rotary regenerative heat exchanger, including large steam-boiler air preheaters. In the presented study the model was used to calculate the fraction of CO_2 and the temperature distributions at the flue-gas outlet of an air preheater. The results show the obvious effects of increased leakage through the radial seals on both parameters. Furthermore, it is shown that combined measurements of the fraction of CO_2 and the temperature at the proposed locations in the outlet channel can provide sufficient information about how well each of the four radial seals is set. The presented monitoring method is also simple enough to be used during everyday operation in power plants.

References

[1] E.J. MacDuff, N.D. Clark, Ljungström air preheater design and operation, Part I: Sealing and Leakage, Combustion 47 (1976) 7–11.
[2] R.K. Shah, T. Skiepko, Influence of leakage distribution on the thermal performance of a rotary regenerator, Appl. Therm. Eng. 19 (7) (1999) 685–705.
[3] T. Skeipko, Indirect estimation of leakage distribution in steam boiler rotary regenerators, Heat Transfer Eng. 18 (1) (1997) 56–81.
[4] T. Skiepko, Method of measuring of seal clearances in rotary heat exchangers and some experimental results, in: J.F. Keffer, R.K. Shah, E.N. Ganic (Eds.), Experimental Heat Transfer, Fluid Mechanics and Thermodynamics 1991, Proc. Second World Conf. Exp. Heat Transfer, Fluid Mech. Thermodyn. June 1991, Dubrovnik, Yugoslavia, Elsevier, New York, 1991.
[5] T. Skiepko, Method of monitoring and measurement of seal clearances in a rotary heat exchanger, Heat Recov. Syst. CHP 8 (1988) 469–473.
[6] T. Skiepko, Some essential principles for adjustment of seal clearances in rotary regenerators, Heat Transfer Eng. 14 (2) (1993) 27–43.
[7] T. Skiepko, Irreversibilities associated with a rotary regenerator and the efficiency of a steam power plant, Heat Recov. Syst. CHP 10 (3) (1990) 187–211.
[8] B. Drobnič, A. Senegačnik, J. Oman, Vpliv netesnosti kotlovskih naprav na njihovo učinkovitost, Strojniški Vestnik, letnik 45 (št. 2) (1999) 75–84.
[9] B. Franković, Analiza izmjene topline u suhom rotirajućem regeneratoru topline, Strojarstvo 35 (3–4) (1993) 111–120.
[10] J.F. Wendt, Computational Fluid Dynamics, second ed., Springer-Verlag, Berlin, 1996.
[11] J.A. Stasiek, Experimental studies of heat transfer and fluid flow across corrugated-undulated heat exchanger surfaces, Int. J. Heat Mass Transfer 41 (6–7) (1998) 899–914.
[12] J. Stasiek, M.W. Collins, M. Ciofalo, P.E. Chew, Investigation of flow and heat transfer in corrugated passages – I. Experimental results, Int. J. Heat Mass Transfer 39 (1996) 142–164.
[13] I. Kuštrin, B. Drobnič, J. Oman, M. Tuma, M. Čefarin, Cylindrical probe for simultaneous single-point measurment of gas composition, velocity and temperature. Short-term patent: publication no. 20946. Slovenian Intellectual Property Office, Ljubljana, 2003.
[14] Wärmetechnische Abnahmeversuche an regenerativen Luft- und Abgasvorwärmern, Einfache Luftvorwärmer, VDI 3921, December 1994.
[15] B. Drobnič, J. Oman, I. Kuštrin, U. Rotnik, Optimizing the locations of the measuring points for an online calculation of the exhaust flue-gas loss, Forschung im Ingenieurwesen, vol. 69, Springer-Verlag, 2005, 76–81.